Theoretical research on a multi-beam modulated electron gun based on carbon nanotube cold cathodes

Xuesong Yuan, Bin Wang, Matthew T. Cole, Yu Zhang, Shaozhi Deng, William I. Milne & Yang Yan

Abstract—Multi-beam modulation in a carbon nanotube (CNT) cold cathode electron gun is herein investigated in order to develop miniaturized and fully-integrated vacuum electron devices. By exposing the electron source to a millimeter-wave signal the steady state field emission current density is efficiently modulated by the incident high-frequency (HF) electric field. Our simulation results of this multi-beam electron gun show that the field emission current density can be efficiently modulated by different incident frequency millimeter-waves. We find that the modulation depth is increased by enhancing the HF input power and anode operation voltage. The modulation frequency and phase of each electron beam can be controlled using a single millimeter-wave source and by simply adjusting the lateral distance between adjacent CNT cold cathodes.

Keywords—carbon nanotube; cold cathode; electron gun;

I. Introduction

Due to their high power and high frequency operation, vacuum electron radiation sources underpin radar, communication, and particle accelerator systems [1]. Nevertheless, large working volumes, high temperature operation, and slow reaction times, due to the need for thermionic cathodes, has limited the application of vacuum electron radiation sources in some fields. Solid-state electron radiation sources have gleaned increasing attention of late. They have developed rapidly and have replaced their vacuum counterparts in many applications. Their simple miniaturization, low working voltages, room temperature operation, and ready integration are particularly attractive. However, solid-state electron radiation sources have some limitations; their poor anti-interference performance, deleterious responsiveness to incident radiation, and low output power in the millimeter-wave and terahertz frequency bands are perhaps some of the most critical issues plaguing solid-state radiation sources to date. Vacuum microelectronic (VME) devices combine vacuum and solid-state electronics[2]. They have many advantages inherited from both the vacuum and solid-state electron devices upon which they are based, including high frequency operation, low-temperature operation and simple integration. Central to such VME radiation sources is the derivation of a room temperature, rapidly time-responding electron beam based on field emission cold cathode sources. CNTs have proven a leading field emission material[3]. Such nanoengineered devices mediate high emission current densities, impressive chemical stability, mechanical strength and temporal stability[4], making CNTs well-suited to underpin the next generation of VME radiation sources[5-9].

To develop integrated VME radiation source, there are two key technologies requiring consideration. First of which is the effective beam-wave interaction. VME devices are often small in volume (typically of under the order of $1cm^3$) whilst the electron beam velocity is near relativistic. In such a regime the limited interaction time makes it challenging to impart high energy densities from the HF field to the emerging modulated electron beam. Traditional vacuum electron devices have shown that if the HF field interacts with a prior-modulated electron beam, the beam-wave interaction efficiency will be improved somewhat as a result[10-12]. Therefore, it is very important to develop means of modulating the source electron beam prior to HF field exposure. Secondly, frequency and phase synchronization of each radiation source is evidently a key challenge to be resolved. Different frequency radiation sources are often difficult to integrate within single package. For phase-unsynchronized same-frequency radiation sources, phase-coherency problems often arise which dramatically reduces the functionality of the integrated VME radiation sources.

In this paper we develop a multi-beam modulated CNT cold cathode electron gun towards realizing a fully-integrated VME radiation source. Firstly, a modulation method is proposed based on conventional field emission theory[13-14]. In this first instance the field emission beam is wholly modulated by the HF field confined within the cavity. We find that the power of electron beam is low and the modulation phase of the different emerging beams lacks control. In this method, both the electrostatic field and HF field act concurrently on the CNT cold cathode. A modulated electron beam is generated, even when the millimeter-wave

This work was supported by the National Basic Research Program of China (No.2013CB933603) and National Natural Science Foundation of China (No.U1134006, No.61101041).

Xuesong Yuan, Bin Wang & Yang Yan are with the School of Physical Electronics, University of Electronic Science & Technology of China, Chengdu 610054 China (e-mail: yuanxs@uestc. edu.cn).

Matthew T. Cole & William I. Milne are with the Department of Engineering, Electrical Engineering Division, Cambridge University, CB3 0FA, United Kingdom(e-mail: mtc35@cam.ac.uk).

Yu Zhang & Shaozhi Deng are with the State Key Laboratory Optoelectronic Materials & Technologies, Sun Yat-Sen University, Guangzhou 510275 China(e-mail: stsdsz@mail.sysu.edu.cn).

input power is very weak (<1W). The electron beam power can be significantly improved by increasing anode operation voltage (>1W/100V). In the second part of the paper, we show how entire electron beams can be modulated by the same HF field, thereby allowing for the modulation frequency and phase of each electron beam to be controlled to solve the above integration problem allowing us to realize novel VME radiation sources.

II. Modulation Theory

The field emission current density(J) is given by simplified Fowler-Nordheim equation, of the form:

$$J = AE^2 \exp(-\frac{B}{E}) \tag{1}$$

Where E is the local electric field, and A and B are the approximate Fowler-Nordheim constants. When the electric field includes a varying time-domain component: $E(t)=E_0+E_1(t)$. Here E_0 is the direct current(DC) electrostatic field, $E_1(t)$ is the HF field and $|E_1(t)| << |E_0(t)|$.

Eq.(1) now gives:

$$\begin{aligned} J(t) &= AE^2(t)\exp\left[-\frac{B}{E(t)}\right] \\ &= A\left[E_0+E_1(t)\right]^2 \exp\left[-\frac{B}{E_0+E_1(t)}\right] = \ldots = J_0 + J_1(t) \end{aligned} \tag{2}$$

Based on Eq.(2), we find that the field emission beam current density is composed of two terms; one is the DC component (J_0), and the other is the alternating current(AC) component (J_1). Figure 1 shows the field emission beam current density as a function of electric field in the non-limited emission regime. With the superposition of a HF field $E_1(t)$ a time-modulated current density $J_1(t)$ is obtained. For an increased E_0, and maintained source $E_1(t)$, different resulting J_1 and J_2 AC components, and hence modulation depths, are obtained. When the electrostatic field is larger, the AC current density component is greater. The magnitude of the DC source amplifies the AC output.

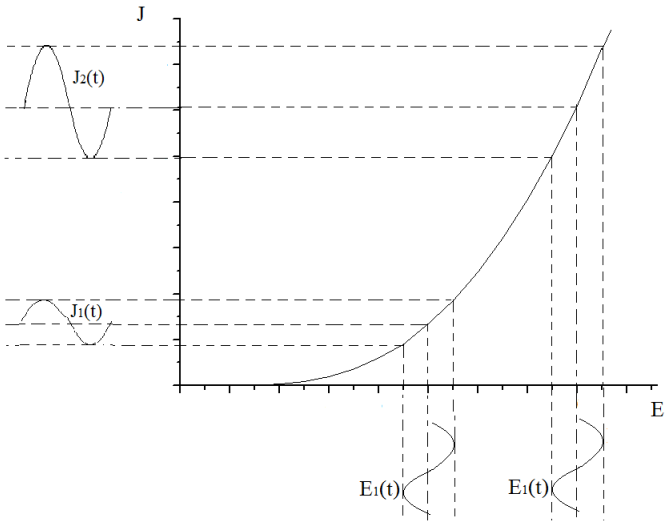

Fig. 1 Field emission beam current density as a function of electric field during DC-shifted AC excitation

III. Multi-beam Modulation Electron Gun

In this section a high modulation efficiency CNT cold cathode electron gun is investigated using 3D electromagnetic simulation software CST. The proposed device includes a HF field input and output structure which act on the CNT electron sources. In the latter part of this section the modulation of a single electron gun is simulated. Finally, the modulation frequency and phase control of differing beams is considered in this CNT cold cathode electron gun structure by CST.

A. Modulating HF CNT electron gun device geometry

In order to obtain high efficiency modulation, the direction of the HF electric field should aligned with the electrostatic field vector. In the present device we have selected a parallel plate geometry, denoted anode and cathode in Fig.2, which is similar to a traditional microstripline. The conducting strip (upper plate) is the perforated anode and the CNT is located on the lower plate, which is the cathode. Both the electrostatic and HF fields lies perpendicular to the anode-cathode structure. The HF field is transmitted in the parallel plate structure with a TME mode.

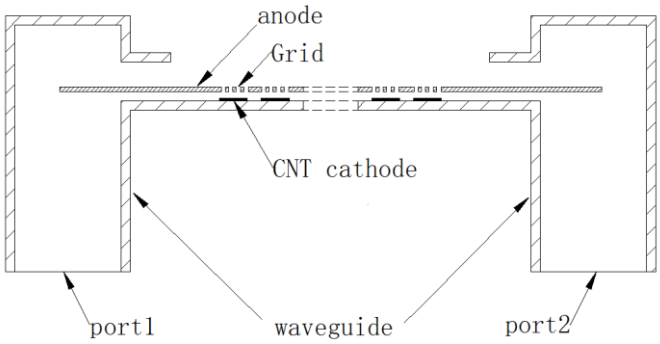

Fig. 2 Scheme of modulated multi-beam CNT cold cathode electron gun

Figure 2 depicts the modulated multi-beam CNT cold cathode electron gun scheme. The HF field is transmitted into the inter-electrode gap from port1 of the rectangular waveguide. The TE_{10} mode of the HF field in the rectangular waveguide is converted to a TEM mode within the parallel plate structure and subsequently passes the linear array of CNT cold cathodes. The HF field exits from port2 on the right side of the waveguide. The lower plate is connected to the waveguide upon which the CNT cathodes are fixed. When the electron gun operates, the anode is set at high DC potential resulting in a time-stable field emission DC current. A HF field is then introduced, propagating along the waveguide, and interacting with the CNT cold cathodes within the TEM mode of the inter-electrode gap. The time-stable electron beams are thusly modulated. Through grid holes in the anode, modulated electron beams are emitted. To ensure minimal leakage the anodes laser-cut grid holes are smaller than the wavelength of HF field.

Figure 3 shows, for perturbations about a nominally 3mm (100GHz) HF field, the simulated S-parameters and electric field vector across the source cross-section. Here the input and output waveguides are WR_{10} (a × b=2.54 × 1.27mm), which is modelled as lossy copper. The width of the lossy steel anode is 0.5mm. The anode is fixed to the cathode by two dielectric brackets. The distance between the anode and cathode is 0.1mm. Our simulation results show that the HF field transmits well in the range of 90-110GHz via the TEM mode in the inter-electrode gap, with a maximum insertion loss of about -0.7dB.

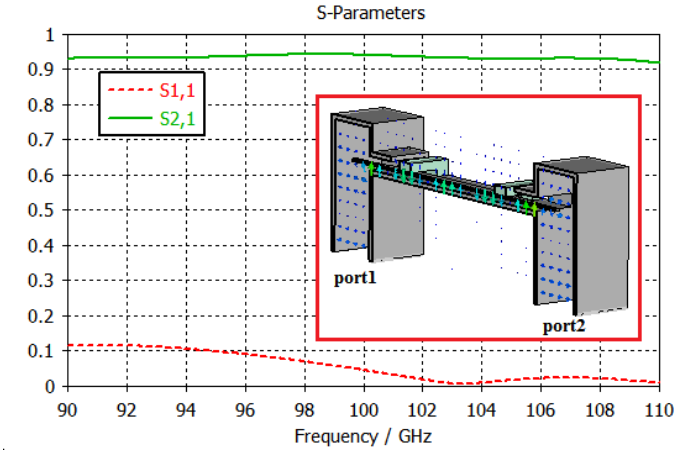

Fig. 3 S11 and S21-parameters of the HF modulation structure. Inset depicts HF electric field vector across the source waveguide cross section

B. Single-beam modulated electron gun

In this section a single-beam modulated electron gun is further studied in the range of 90GHz to 110GHz. Figure 4(a) shows the structure of the electron gun and the resultant electron trajectories. The gun consists of an array of 5×5 CNT cold cathodes, each unit being 0.05×0.05mm. The height of the CNTs is 3 μm. The distance between adjacent unit centers is 0.075mm. To ensure a high anode electron transparency an array of 5×5 apertures is integrated into the anode. The aperture geometry is congruent with the CNT unit layout, except for each unit being 0.06×0.06mm. In our CNT field emission simulations we employ the experimental model, as in [15]. Based on Equation (1), A and B can be obtained by numerical fitting based on our earlier experimental results[16-17].We find experimental that A= $2.8\times10^{-8} A/V^2$, and B= $2.29\times10^{7} V/m$. The input power from the HF field is 5W. Simulation results show that anode grid beam transparency is up to 99%, as shown in Fig. 4(b). We find that the modulation depth of the collector current (11.7-15.2mA) in Fig4(b) is larger than the emission current at an operational voltage of 1000V (12.3-14.8mA) (Fig4(c)). We attribute this to the fact that the emitted electrons are simultaneously accelerated by the HF and electrostatic field, though there nevertheless remains a certain population which presents a varied velocity range. If the size of aperture is increased, the beam transparency of the grid will reach 100%. However, this is at the expense of the surface electric field, which will become increasingly weak for increasing aperture diameter. The electric field incident at the cathode surface center will, in the present optimal geometry, be reduced by some 46%. Such field reduction is common to gated field emission cold cathodes. To counteract this reduction at the cathode center, we are investigating different CNT bundle geometries in order to mediate high enhancement factors [18].

Figure 4(c) shows the electron beam modulated by a 100GHz HF field under different DC operation voltages. For DC operation voltages (U_0) of 600, 800 and 1000V, the electron beam currents, I_0, are 0.97, 4.79 and 13.58mA, respectively (for $0 < t \leq 0.02$ns). For $t \leq 0.02$ns, as the HF field has not as yet reached the CNT cathodes, the DC beam current remains largely unchanged and time-invariant. For t>0.02ns, the HF field begins to modulate the electron beam and the resulting amplitude modulation (under different DC operation voltages) is given by $\Delta I=(I_{max}-I_{min})/2$ and is 0.2, 0.6 and 1.25mA, respectively. The modulation currents are increased with increasing DC operation voltage. Further simulations show that if we increase the HF input power the modulation current also increases. Figure 4(d) illustrates how the electron beam is modulated by different HFfrequencies. For a single CNT cathode, we note that the amplitude modulation for different frequency HF fields is almost invariant with HF frequency under standard operating conditions (P_{in}= 5W, U_0= 1000V).

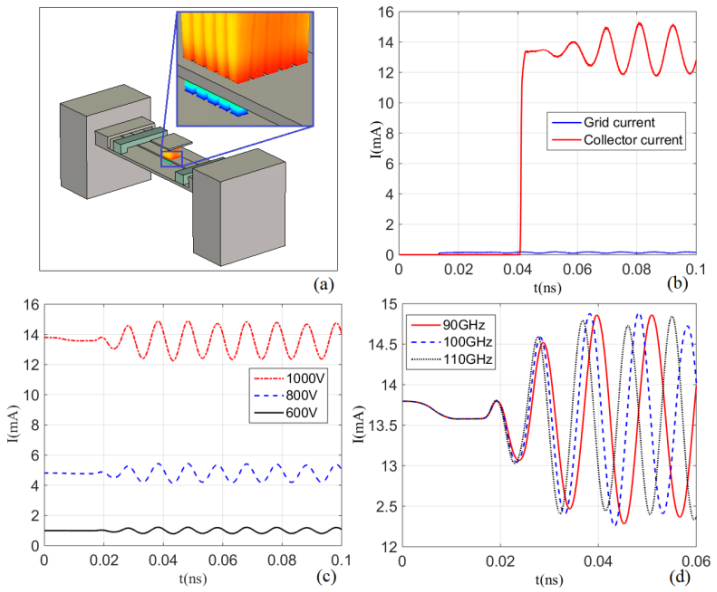

Fig.4 CNT cathode single-beam modulation. (a) Structure of the electron gun. Inset: resulting electron trajectories. (b) Grid current and collector current. (c) Modulated beam current as a function of DC operation voltage. (d) Beam current amplitude modulation as a function of HF field frequency (P_{in}= 5W, U_0= 1000V).

C. Modulation frequency and phase control in a multi-beam electron gun

In this section the distribution of the HF field within the multi-beam electron gun is analyzed. We then consider means of regulating the modulation frequency and phase control of

the multi-beam system. Herein we investigate a nominally five-beam system, where all the beams are in phase with each other, and all of which operate at a single frequency.

Figure 5(a) shows the structure of the multi-beam HF modulated source. The absolute value of the normalized HF electric field $\bar{E}_n$, aligned parallel to the direction of propagation, is shown in figure 5(b). Three principal frequencies are considered; 94, 100 and 106GHz. The half-wavelength of the HF field along the transmission direction, $L_{\lambda/2}$, for the three frequencies regimes considered, is $L_{\lambda/2}^{94}=1.57mm$, $L_{\lambda/2}^{100}=1.49mm$, $L_{\lambda/2}^{106}=1.41mm$. Based on $L_{\lambda/2}$ we set the distance between two adjacent CNT cathodes, allowing geometric control over the beam modulation depth due to engineered intra-beam interference. When the distance between two CNT cathodes is equal to $(2n+1)L_{\lambda/2}, n=1,2,3...$, the modulation phase is equal and opposite. When the distance between two adjacent CNT cathodes is equal to $2nL_{\lambda/2}, n=1,2,3...$, the modulation phase is equal for all the emitters. As $L_{\lambda/2}$ is frequency dependent and there are multiple beams along the HF fields direction of propagation, the phase difference between various modulation frequencies will manifest if we set the source to operate at a fixed mid-frequency of 100GHz with $L_{\lambda/2}^{100}$ =1.49mm. Considering this case, if the phase compensation for different frequencies cannot be achieved, we ultimately limit the modulation frequency range and the number of electron beams (and hence total output power).

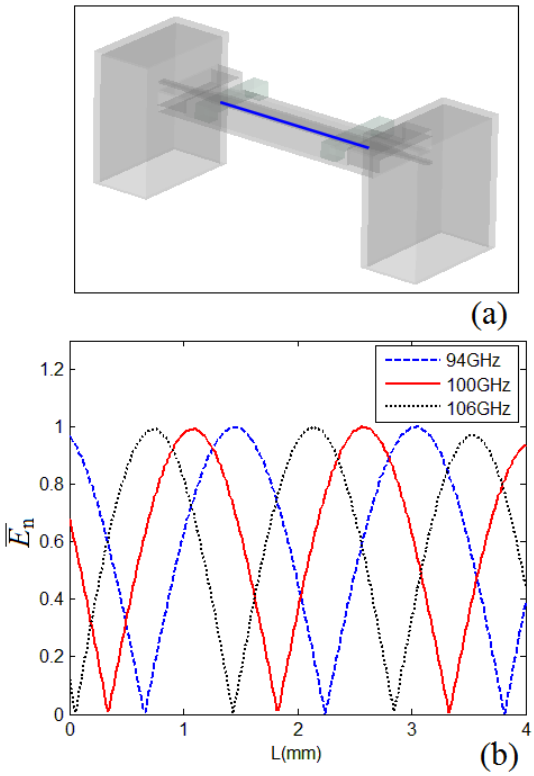

Fig. 5 (a)Structure of the multi-beam HF modulated source. (b) Absolute normalized HF electric fields along indicated blue cross section as in figure 5(a).

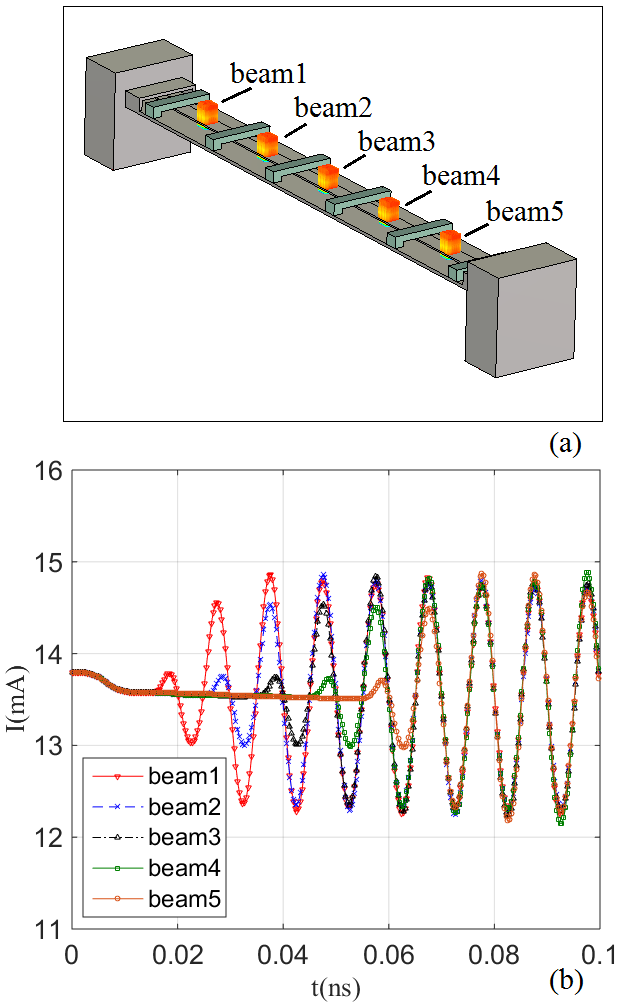

Fig. 6 A five-beam modulated CNT cold cathode electron gun. (a) Scheme depicting the electron gun structure and resulting electron trajectories. (b) Electron beam currents from each of the five electron sources, as a function of time, for a modulation frequency of 100GHz.

In the five-beam electron gun system the size of each CNT cathode is about 0.4mm. As a result we have physically limited the maximum distance between different frequencies bands to $D_{\max}=5\times\left|L_{\lambda/2}^{f1}-L_{\lambda/2}^{f2}\right|$, which should be <0.4mm, where f_1 denotes the mid-frequency and f_2 is the minimum/maximum frequency. When the modulation mid-frequency is 100GHz, the modulation frequency range is from 94 to 106GHz. Here the distance between two adjacent CNT cathodes is 2.98mm. Figure 6(a) shows the structure of the electron gun and the five electron beam trajectories under these operating conditions. Each electron beam is generated from a 5×5 CNT array where all other geometric parameters are the same as those in the earlier single-beam modulation system. Figure 6(b) shows the beam current for the five electron beams, as a function of time, for a modulation frequency of 100GHz. Initially the five electron beam currents are all 13.58mA as there is no HF field. When

t=0.015ns, the first beam is modulated. when *t*=0.025ns, the second beam is modulated, where the modulation phase of the second beam is equal to that of the first beam. The following three beams are subsequently modulated successively. When t=0.07ns, the modulation of the five beams achieves a steady state condition, with all five beams being in phase.

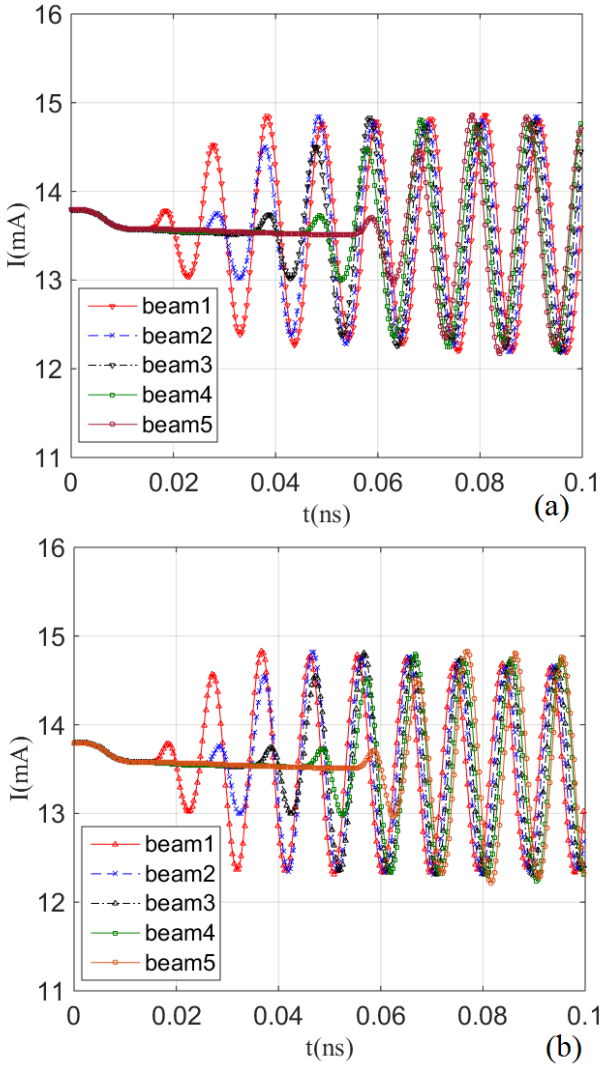

Fig. 7 Broadband modulation of the five-beam CNT cold cathode electron gun. Five-beam current variation with time for (a) 94GHz and (b) 106GHz HF fields.

To realize broadband frequency modulation, the 94 and 106GHz cases have been simulated in the five-beam CNT cold cathode electron gun. Figure 7(a) shows the beam currents for the five electron beams modulated at a HF field of 94GHz. Note that the modulation sequence of the five beams is the same as that of 100GHz case and that the five beam modulation frequency is also equivalent. If the phase of beam 3 is set as the center phase. The phase of between beams 3 and 1 or between beams 3 and 5 have only a very slight difference ($<\pm 0.05\pi$), which our studies show is largely negligible as it pertains to the device operation. Figure 7(b) shows five electron beams modulated by a 106GHz HF field. As $L_{\lambda/2}^{106}$ is smaller, the phase difference for beams 3,1 or beams 3,5 are larger than that of the 94GHz modulation. Nevertheless, it remains comparatively small ($<\pm 0.06\pi$). Further simulations have shown that the phase difference of two beams tends to decrease as the modulation frequency tends to 100GHz. We can therefore, in the present device geometry, effectively adjust the modulation frequency range according to vacuum devices functional requirements.

IV. Conclusion

Here we have studied the high frequency modulation of the DC field emission current density from carbon nanotube based cold cathode radiation sources in order to develop miniaturized and highly integrated vacuum electron devices. The studied geometry allows for an increased modulation depth by increasing the HF field input power in addition to the driving electrostatic field. By controlling both the HF field and electrostatic field we have demonstrated a viable means of high power electron beam modulation. The modulated electron beam can be used not only to interact with the output modulated HF field, realized millimeter-wave amplification, but also to stimulate terahertz oscillator via frequency multiplication in a resonant cavity.

A methodology to control the modulation frequency and phase in a linear multi-beam CNT field emission electron gun has been outlined. The detailed modulated electron beams allow stimulation of different millimeter-wave/terahertz radiation sources, the frequency and phase of which will be locked, thereby allowing for fully-integrated vacuum radiation sources. Broadband modulation and amplification have been realized which offer a means to develop next generation communications amplifiers based on emerging nanocarbon materials.

References

[1] Robert J.Barker, Edl Schamiloglu, High-power Mircowave Sources and Technologies, Wiley-IEEE Press, 2001.

[2] W. Zhu, *Vacuum Microelectronics*, John Wiley & Sons, 2001.

[3] Clare M. Collins, Richard J. Parmee, William I. Milne and Matthew T. Cole, "High Performance Field Emitters,"*Advanced Science*, 1500318, Feb. 2016

[4] Baughman R H, Zakhidov A A, De Heer W A. "Carbon nanotubes—the route toward applications.*Science*," 297(5582): 787-792,2002.

[5] F. Brunetti, R. Riccitelli, A. D. Carlo, A. Fiori, S. Orlanducci, V. Sessa, M. L. Terranova, M. Lucci, V. Merlo, and M. Cirillo, "Flip-cathodedesign for carbon nanotube-based vacuum triodes," *IEEE Electron Device Lett.*, vol. 29, no. 1, pp. 111–113, Jan. 2008.

[6] Giacomo Ulisse, Francesca Brunetti, Emanuela Tamburri, Silvia Orlanducci,Matteo Cirillo, Maria Letizia Terranova, and Aldo Di Carlo,"Carbon Nanotube Cathodes for Electron Gun,"*IEEE Trans. Electron Dev.Let.*, vol. 34, no. 5, may 2013

[7] G. Ulisse, F. Brunetti, and A. D. Carlo, "Study of the influence of transverse velocity on the design of cold cathode-based electron guns for terahertz devices," *IEEE Trans. Electron Dev.*, vol. 58, no. 9,pp. 3200–3204, Sep. 2011.

[8] H. M. Manohara, R. Toda, H. R. Lin, A. Liao, M. J. Bronikowski,and P. H. Siegel, "Carbon nanotube bundle array cold cathodes for THz vacuum tube sources," *J. Infr., Millim., Terahertz Waves*, vol. 30,pp. 1338–1350, Jul. 2009.

[9] H. J. Kim, J. J. Choi, J.-H. Han, J. H. Park, and J.-B. Yoo, "Design and field emission test of carbon nanotube pasted cathodes for travelingwave tube applications," *IEEE Trans. Electron Dev.*, vol. 53, no.11, pp. 2674–2680, Nov. 2006.

[10] John H. Booske, Richard J. Dobbs, Colin D. Joye, Carol L. Kory, George R. Neil, Gun-Sik Park, Jaehun Park, and Richard J. Temkin, *Vacuum Electronic High Power Terahertz Sources*, IEEE Transactions on Terahertz Science and Technology, Vol.1, No.1, 54-75, 2011

[11] Craig B. Wilsen, Yue Ying Lau, David P. Chernin, Ronald M. Gilgenbach, *A Note on Current Modulation From Nonlinear Electron Orbits*, IEEE Transactions on Plasma Science, Vol. 30, No. 3, 1176-1178, 2002

[12] Sergei A. Kitsanov, Alexei I. Klimov, Sergei D. Korovin, Boris M. Kovalchuk, Ivan K. Kurkan, Sergey V. Loginov,Igor V. Pegel, Sergei D. Polevin, Sergei N. Volkov, and Andrey A. Zherlitsyn, *S-Band Vircator With Electron Beam Premodulation Based on Compact Pulse Driver With Inductive Energy Storage*, IEEE Transactions on Plasma Science, Vol. 30, No. 3, 1179-1185, 2002

[13] K. B. K. Teo, E. Minoux, L. Hudanski, F. Peauger, J.-P. Schnell,L. Gangloff, P. Legagneux, D. Dieumegard, G. A. J. Amaratunga, and W. I. Milne, "Microwave devices: Carbon nanotubes as cold cathodes,"*Nature*, vol. 437, no. 7061, p. 968, Oct. 2005.

[14] P. Legagneux, N. Le Sech, P. Guiset, L. Gangloff, C. Cojocaru, JP Schnell, D. Pribat, K.B.K. Teo J. Robertson, W.I. Milne,F. André, Y. Rozier and D. Dieumegard,"Carbon nanotube based cathodes for microwave amplifiers,"IEEE International Vacuum Electronics Conference, pp.80-81, April 2009.

[15] Chi Li1,Yan Zhang, Mark Mann, David Hasko, Wei Lei, Baoping Wang, Daping Chu, Didier. Pribat, Gehan A. J. Amaratunga and William I. Milne,"High emission current density, vertically aligned carbon nanotube mesh, field emitter array," Appl. Phys. Lett. 97, 113107, 2010

[16] Yuan Xue-Song, Zhang Yu, Sun Li-Min, Li Xiao-Yun,Deng Shao-Zhi,Xu Ning-Sheng,Yan Yang,"Study of pulsed field emission characteristics and simulation models of carbon nanotube cold cathodes,"*Acta Phys. Sin.* vol. 61, no. 21, 216101, Nov. 2012.

[17] Xuesong Yuan, Yu Zhang, Huan Yang, Xiaoyun Li, Ningsheng Xu, Shaozhi Deng, and Yang Yan,"A Gridded High-Compression-Ratio CarbonNanotube Cold Cathode Electron Gun," *IEEE Electron Device Lett.*,vol.36, No.4, pp.399-401, April 2015.

[18] Matthew. T. Cole, Ken B. K. Teo, Oliver Groening, Laurent Gangloff, Pierre Legagneux, & William I. Milne, "Deterministic Cold Cathode Electron Emission from Carbon Nanofibre Arrays" *Nat. Sci. Rep.*, Vol. 40, pp. 4840, 2014.